Analytical Methods

DOI: 10.1002/anie.201408985

Photoswitching Kinetics and Phase-Sensitive Detection Add Discriminative Dimensions for Selective Fluorescence Imaging**

Jérôme Querard, Tal-Zvi Markus, Marie-Aude Plamont, Carole Gauron, Pengcheng Wang, Agathe Espagne, Michel Volovitch, Sophie Vriz, Vincent Croquette, Arnaud Gautier, Thomas Le Saux,* and Ludovic Jullien**

Abstract: *Non-invasive separation-free protocols are attractive for analyzing complex mixtures. To increase selectivity, an analysis under kinetic control, through exploitation of the photochemical reactivity of labeling contrast agents, is described. The simple protocol is applied in optical fluorescence microscopy, where autofluorescence, light scattering, as well as spectral crowding presents limitations. Introduced herein is OPIOM (out-of-phase imaging after optical modulation), which exploits the rich kinetic signature of a photoswitching fluorescent probe to increase selectively and quantitatively its contrast. Filtering the specific contribution of the probe only requires phase-sensitive detection upon matching the photoswitching dynamics of the probe and the intensity and frequency of a modulated monochromatic light excitation. After in vitro validation, we applied OPIOM for selective imaging in mammalian cells and zebrafish, thus opening attractive perspectives for multiplexed observations in biological samples.*

Measuring the concentration of a specific analyte in systems as complex as biological or medical samples remains a great challenge, in particular if the sample has to remain in its native state (e.g. living cells). In this context, non-invasive methods such as fluorescence microscopy have to be adopted. When one images fluorescent probes in cells,[1] contrast mainly results from the high brightness of the probe, which enables one to obtain a high signal to background ratio as long as the probe concentration is large enough and as long as the autofluorescence and light scattering of the medium is not too high. Other photophysical properties enable one to further distinguish fluorescent species. The one traditionally used for multiplexing is the emission wavelength. However only three or four probes can be distinguished using appropriate band pass filters since emission bands are rather broad and tend to overlap (spectral crowding).

Detecting individual emitters with similar emission properties thus requires efficient discrimination strategies. Time-gated detection is relevant if the fluorescence lifetimes of the emitters are sufficiently different,[2] but this is often challenging to achieve with the fluorescent proteins/probes commonly used in biology as they mostly display lifetimes within the same short nanosecond range. Hence imaging techniques exploiting the photochemical reactivity of photoswitchable fluorescent probes have been proposed to enhance contrast among fluorescence emitters. Optical lock-in detection[3,4] (OLID) images the correlation coefficient between the total fluorescence emission and an external reference signal from the photoswitchable fluorescent target over several cycles of dual-wavelength-driven optical switching. Synchronously amplified fluorescence image recovery[5–12] (SAFIRe) images the amplitude of the fluorescence modulation resulting from modulating a secondary light source, which depopulates long-lived dark states of the fluorescent probe.

[*] J. Querard, M.-A. Plamont, P. Wang, Dr. A. Espagne, Dr. A. Gautier, Dr. T. Le Saux, Prof. Dr. L. Jullien
École Normale Supérieure—PSL Research University
Department of Chemistry, 24 rue Lhomond, 75005 Paris (France)
E-mail: Arnaud.Gautier@ens.fr
Thomas.Lesaux@ens.fr
Ludovic.Jullien@ens.fr

J. Querard, M.-A. Plamont, P. Wang, Dr. A. Espagne, Dr. A. Gautier, Dr. T. Le Saux, Prof. Dr. L. Jullien
Sorbonne Universités, UPMC Univ Paris 06, PASTEUR
75005 Paris (France)

J. Querard, M.-A. Plamont, P. Wang, Dr. A. Espagne, Dr. A. Gautier, Dr. T. Le Saux, Prof. Dr. L. Jullien
CNRS, UMR 8640 PASTEUR, 75005 Paris (France)

Dr. T.-Z. Markus, Dr. V. Croquette
École Normale Supérieure, Département de Physique and Département de Biologie, Laboratoire de Physique Statistique UMR CNRS-ENS 8550, 75005 Paris (France)

C. Gauron, Prof. Dr. M. Volovitch, Prof. Dr. S. Vriz
Centre for Interdisciplinary Research in Biology (CIRB) CNRS UMR 7241/INSERM U1050/Labex MemoLife
PSL Research University/Collège de France, Paris (France)

C. Gauron, Prof. Dr. S. Vriz
Université Paris Diderot Sorbonne Paris Cité, Paris (France)

P. Wang
Institut Curie, Centre de Recherche, UMR 176 CNRS-Institut Curie 26 rue d'Ulm, 75248 Paris (France)

Prof. Dr. M. Volovitch
École Normale Supérieure, Institute of Biology at the Ecole Normale Supérieure (IBENS), CNRS UMR 8197, INSERM U1024, PSL Research University, 75005 Paris (France)

[**] We thank A. Miyawaki and S. Jakobs for providing the genes of Dronpa-3 and Dronpa-2, respectively, and E. Ipendey for her excellent technical assistance. D. Bensimon, M. Dahan, and Z. Gueroui are acknowledged for fruitful discussions. This work was supported by the ANR (France BioImaging, Morphoscope2), CNano Ile de France (Fluoroswitch), and PSL Research University (IMRE-SOLV).

Supporting information for this article is available on the WWW under http://dx.doi.org/10.1002/anie.201408985.

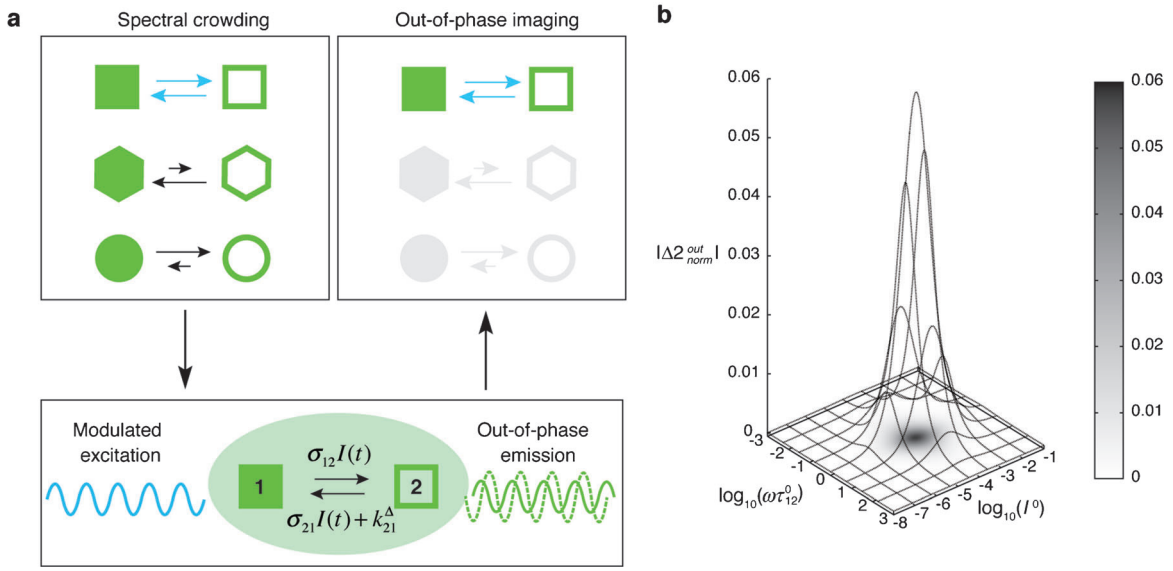

Figure 1. a) Out-of-phase imaging after optical modulation (OPIOM). A periodically modulated light generates modulation of the signal from photoswitchable fluorescent probes exchanging between two states (**1** and **2**), each having a different brightness. The image of a targeted probe is selectively and quantitatively retrieved from the amplitude of the out-of-phase component of the fluorescence emission at angular frequency (ω) upon matching I^0 and ω to its dynamic parameters (σ_{12}, σ_{21}, k^{Δ}_{21}). b) Theoretical response of a photoswitchable fluorophore, **1**⇌**2**, submitted to light harmonic forcing of small amplitude. The absolute value of the normalized amplitude of the out-of-phase oscillations in concentration of **2**, $|\Delta 2^{out}_{norm}|$, is plotted versus the light flux I^0 (in ein s^{-1} m^{-2}) and the adimensional relaxation time $\omega\tau^{0}_{12}$. See Equation (18) and supplementary text 1 in the Supporting Information. $\sigma_{12} = 73\ m^2\ mol^{-1}$, $\sigma_{21} = 84\ m^2\ mol^{-1}$, $k^{\Delta}_{21} = 1.5\times10^{-2}\ s^{-1}$.

Herein, we exploit the unique discriminative kinetic parameters[13,14] of photoswitchable fluorescent probes to explore an alternative approach for selective and quantitative imaging. Our strategy relies on a periodically modulated monochromatic illumination with average light intensity and modulation frequency tuned so that the amplitude of the out-of-phase fluorescence response extracted from phase-sensitive detection results only from a fluorescent probe of interest, thus enabling extraction of its signal from a complicated fluorescence signal composed of several emitters. Our strategy notably differs from OLID and SAFIRe by its use of a single modulated light source whose average intensity and frequency depend on easily predictable resonant conditions, and by the exploitation of the phase lag between the modulated excitation and the fluorescence response. Our experimental set-up is correspondingly low cost and the acquisition protocol is simple and robust.

We first discuss the principle of our strategy and the analysis which enables selective detection (see supplementary text 1 in the Supporting Information). We consider a photoswitchable fluorophore **P** which exhibits two states of different brightnesses: state **1**, which is thermodynamically stable and state **2**, which is generated upon illumination (Figure 1 a). Note that this model applies for any photoactive system in which the kinetic behavior is dynamically reduced to light-driven exchanges between two states (see supplementary text 2).[2,15,16] Discrimination relies on the triplet of dynamic parameters (σ_{12}, σ_{21}, k^{Δ}_{21}) which characterize **P**, where σ_{12} and σ_{21} are the molecular action cross-sections of the forward and backward photochemical processes, and k^{Δ}_{21} is the rate constant of the thermal resetting. This discrimination is accomplished by using a periodically modulated monochromatic light excitation (average intensity I^0, fundamental angular frequency ω, modulation amplitude α), which forces the concentrations of the states **1** and **2** to oscillate with orthogonal in- and out-of-phase components exhibiting (σ_{12}, σ_{21}, k^{Δ}_{21})-dependent amplitudes. We apply phase-sensitive detection and focus on the amplitude of the out-of-phase first-order term $\Delta 1^{out} = -\Delta 2^{out}$ which reports on concentration oscillations at the angular frequency ω (see Figure S1). One can analytically show that this out-of-phase term in the concentration profile (proportional to the total concentration of **P** and easily retrieved from the fluorescence intensity) can be univocally maximized when the control parameters of illumination (I^0, ω) match the following simple resonance conditions in the space of the dynamic parameters [Equation (1); see also Figure 1 b].

$$I^0 = \frac{k^{\Delta}_{21}}{\sigma_{12}+\sigma_{21}}; \quad \omega = 2k^{\Delta}_{21} \tag{1}$$

Conversely, the out-of-phase amplitude rapidly vanishes when (I^0, ω) diverge from these values (Figure 1 b). These resonance conditions are not significantly affected by photobleaching (see supplementary text 3). Importantly, the above resonance conditions maximize the out-of-phase response of **P**, but not that of another photoswitchable fluorophore, **X**, characterized by a different triplet of parameters ($\sigma_{12,X}$, $\sigma_{21,X}$, $k^{\Delta}_{21,X}$).

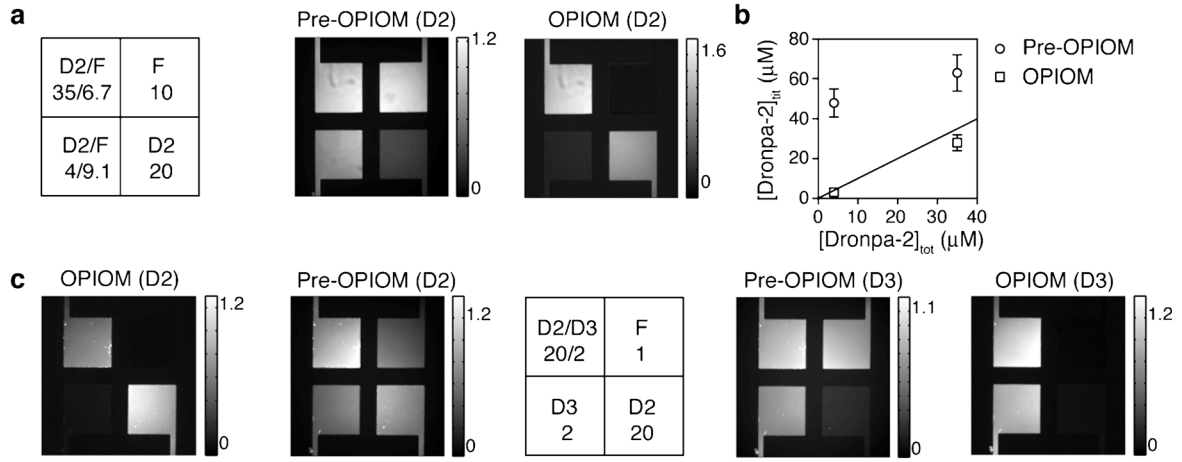

Figure 2. OPIOM validation in a microfluidic device composed of four chambers as described in the scheme (the numbers indicate the concentrations in μM). a) Selective imaging of Dronpa-2 (D2) against fluorescein (F). b) Titration of Dronpa-2 ($[\text{Dronpa-2}]_{tit}$) calculated from the pre-OPIOM (circle) and OPIOM (square) images in (a). The line shows the expected Dronpa-2 concentrations ($[\text{Dronpa-2}]_{tot}$). c) Selective imaging of Dronpa-2 and Dronpa-3 (D3). The microfluidic device was imaged using a sinusoidal light modulation of small amplitude tuned either to the resonance of Dronpa-2 (a,c) or Dronpa-3 (c). Images labeled Pre-OPIOM and OPIOM correspond to respectively the unfiltered and OPIOM-filtered images. $T = 37\,°C$; pH 6.8 MES buffer. See the Supporting Information for details.

These theoretical predictions suggest that out-of-phase imaging after optical modulation (OPIOM;[*] see Figure 1 a) can enable highly selective imaging of a photoswitchable fluorescent target **P** in a mixture of spectrally interfering fluorophores, photoswitchable or not (see Figure S2). First the out-of-phase amplitude of the fluorescence signal does not contain any contribution from non-photoactive fluorescent interfering species, which respond as constant and in-phase terms with the light modulation. In contrast to spectral discrimination, phase discrimination here provides absolute orthogonality. Moreover, among photoswitchable interfering fluorophores, only **P** will display a significant out-of-phase amplitude.

To validate OPIOM experimentally, we used Dronpa-2 (or M159T)[17] and Dronpa-3 (or V157I/M159A).[18] These two variants of the reversibly photoswitchable green fluorescent protein Dronpa,[19] whose chromophore undergoes *cis*-to-*trans* and *trans*-to-*cis* photoisomerization, have been reported to display faster thermal resetting while exhibiting good quantum yields of fluorescence (0.23–0.33 for Dronpa-2[17,18] and 0.28[18] for Dronpa-3; 0.85 for Dronpa[19]). Note that a fast thermal resetting (large k_{21}^{Δ}) improves both the signal to noise ratio (by increasing I^0) and the temporal resolution (by increasing ω) of the imaging protocol (see the resonance conditions above), while a large quantum yield of fluorescence increases the OPIOM signal. In addition, the photochemical properties of these Dronpa mutants are poorly sensitive to environmental changes:[20] at most fourfold changes are expected for both the resonant ω and I^0 upon increasing viscosity, which remains lower than the bandwidth of the resonance (typically one order of magnitude; see Figure 1 b). This insensitivity enables one to benefit from widely applicable resonance conditions for OPIOM-selective detection of Dronpa-2 and Dronpa-3 in various environments.

The resonance conditions are calculated from the sum $\sigma_{12} + \sigma_{21}$ for the cis-to-trans and trans-to-cis photoisomerization action cross-sections and the thermal resetting rate constant k_{21}^{Δ}. Hence, we first submitted Dronpa-2 and Dronpa-3 to a straightforward series of light jump experiments (see supplementary text 4 and Table S1). Photoconversion of Dronpa-2 and Dronpa-3 revealed monoexponential relaxation of the fluorescence signal (see Figure S6), meaning that they both follow the two-state dynamic model underlying the OPIOM theory within the range of light intensity investigated. The $\sigma_{12} + \sigma_{21}$ value was extracted from the light intensity dependence of the relaxation time associated with the photoconversion of **P** upon irradiation (Figure S6): at 37 °C, we found (157 ± 5) and $(21 \pm 3)\ m^2\,mol^{-1}$ for Dronpa-2 and Dronpa-3, respectively. k_{21}^{Δ} was directly obtained by monitoring the fluorescence recovery rate in the dark (see Figure S7), thus yielding $(1.50 \pm 0.05) \times 10^{-2}\ s^{-1}$ and $(0.17 \pm 0.01)\ s^{-1}$ for Dronpa-2 and Dronpa-3, respectively, at 37 °C. The measured kinetic parameters were in good agreement with literature results,[17,18] and were further confirmed by a series of light-modulation experiments (see supplementary text 5 and Figure S8).

To demonstrate OPIOM experimentally, we used a microfluidic device composed of four chambers containing solutions of Dronpa-2 at three different concentrations. The fourth chamber was filled with fluorescein, which is a non-photoactive fluorophore that emits in the Dronpa-2 wavelength range (see Figure S9) but characteristically responds

[*] OPIOM acts much like opium according to Thomas De Quincey in *Confessions of an English Opium-Eater* help long-buried memories resurface "veiled or unveiled, the inscription remains forever, just as the stars seem to withdraw before the common light of day, whereas in fact we all know that it is the light which is drawn over them as a veil, and that they are waiting to be revealed when the obscuring daylight shall have withdrawn".

in-phase to the light modulation. The device was imaged using a classical epifluorescence microscope equipped with a light-emitting diode (LED; see Figure S10), whose intensity, radial frequency, and phase are easily controlled by driving electrical current. The illumination conditions were tuned to the Dronpa-2 resonance conditions. Two separate sets of images were collected: one corresponding to the average fluorescence intensity (hereafter called pre-OPIOM image) and a second corresponding to the processed OPIOM image (see supplementary text 6 and Figure S11a). Dronpa-2 fluorescence emission could be detected in both pre-OPIOM and OPIOM images. In contrast, as expected from the absence of an out-of-phase contribution in its fluorescence emission, fluorescein only gave a signal on the pre-OPIOM image, thus demonstrating the expected selective OPIOM imaging. More precisely, for fluorescein and Dronpa-2 at concentrations of 1 and 20 μM, respectively, the corresponding pre-OPIOM and OPIOM images with 1:1 and 1:200 intensity ratios were obtained. With a precision on phase retrieval of 3×10^{-3} rad, OPIOM imaging could typically enhance contrast of Dronpa-2 contribution against fluorescein by a factor $\chi_{D2/F}=10^2$–10^3 [see Eq. (78) in the Supporting Information] with respect to the pre-OPIOM image. Furthermore the three chambers with Dronpa-2 showed relative intensities directly reflecting their concentration (see Figure S11 b,c), which confirms the theoretical prediction that OPIOM signal is proportional to the probe concentration.

To further confirm this feature, we mixed Dronpa-2 and fluorescein in various ratios so that the resulting mixtures gave similar fluorescence intensities on the pre-OPIOM image (Figure 2 a). The excess fluorescein prevented estimation of the Dronpa-2 concentrations from the pre-OPIOM image, but the associated OPIOM image suppressed the contributions from fluorescein (Figure 2 a) and enabled us to accurately quantify the concentrations of Dronpa-2 in the fluorescein/Dronpa-2 mixtures by using the well containing only Dronpa-2 for concentration calibration [Figure 2 b and Eq. (38) in the Supporting Information]. This result demonstrates the capacity of OPIOM to image Dronpa-2 quantitatively within a mixture containing non-photoactive interfering fluorophores.

We next showed that one could distinguish two photoswitchable fluorophores exhibiting similar fluorescence emission (see Figure S9) as long as their dynamic parameters, $\sigma_{12}+\sigma_{21}$ and k_{21}^{A}, were different enough to give two different resonance conditions. Tuning the illumination to the resonance conditions of either Dronpa-2 or Dronpa-3 led to the contrast enhancements $\chi_{D2/D3}=20$ and $\chi_{D3/D2}=10$, respectively, thus enabling selective imaging of Dronpa-2 in presence of Dronpa-3 and vice versa (Figure 2 c and Figure S12). Therefore, OPIOM can selectively detect a photoswitchable target in a mixture of interfering photoswitchable fluorophores as long as they display different resonance conditions.

To test OPIOM for selective imaging in mammalian cells, we imaged fixed HEK293 cells co-expressing nuclear Dronpa-3 and membrane-localized EGFP using modulated excitation tuned to Dronpa-3 resonance. OPIOM enabled removal the interfering EGFP signal and revealed only a Dronpa-3 signal (Figure 3 a and Figure S13). Note that the acquisition time for each frame can be reduced to one period of light modulation (ca. 20 s for Dronpa-3) without any change in the contrast enhancement (see Figure S14). This feature enables imaging of live cells at a time resolution relevant for the study of biological processes and without any significant photobleaching or detrimental cell alteration (Figure 3 b and Figure S14).

Finally, we validated OPIOM for selective imaging in multicellular organisms, where the autofluorescence of tissues and compartments can strongly interfere. As such a model, we chose the zebrafish embryo, in which the yolk strongly fluoresces in the green, thus rendering it difficult to observe

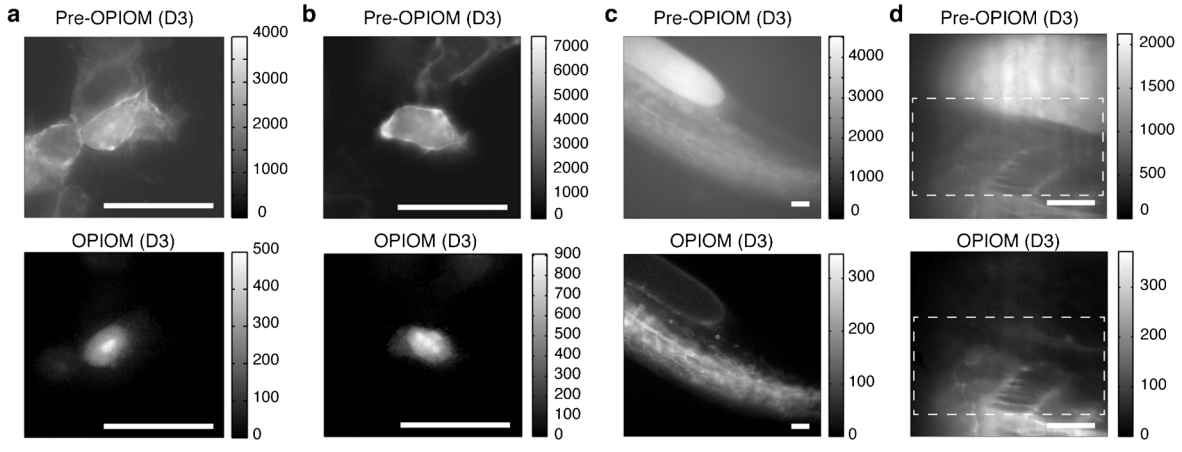

Figure 3. OPIOM application in mammalian HEK293 cells and in 24 hpf zebrafish embryos. a,b) Selective imaging of nuclear Dronpa-3 against membrane-localized EGFP. c,d) Selective imaging of Lifeact-Dronpa-3 against autofluorescence. Fixed (a) or live (b) cells, and zebrafish embryo (c,d) were imaged by epifluorescence (a–c) or single plane illumination microscope (SPIM; d; the dashed rectangles indicate the zone illuminated by the thinnest part of the light sheet) upon illuminating with sinusoidal (a–c) or square wave (d) light modulation of large amplitude tuned on the resonance of Dronpa-3. Images labeled Pre-OPIOM and OPIOM correspond to the unfiltered and OPIOM-filtered, respectively, images. Scale bars represent 50 μm. Experiments were performed either at 37 °C (a–c) or 20 °C (d). See the Supporting Information for details.

the popular green fluorescent probes such as GFP. We injected zebrafish embryos with Lifeact-Dronpa-3 mRNAs for actin targeting and imaged them 24 hours post-fertilization. OPIOM filtered out the yolk autofluorescence and selectively visualized Lifeact-Dronpa-3 in the embryo's tail (Figure 3c).

OPIOM is compatible with light sheet fluorescence microscopy (see Figure S15), which gives access to selective three-dimensional-resolved fluorescence imaging. Thus we selectively imaged Lifeact-Dronpa-3 against a background of autofluorescence (Figure 3d) or GFP-NLS (see Figure S16) in zebrafish embryos.

In conclusion, OPIOM is relevant for selective and quantitative imaging of photoswitchable fluorescent probes. Notably, OPIOM temporal resolution and multiplexing opportunities should benefit from developing bright photoswitchable fluorescent proteins with thermal resetting on the time scale of seconds. This would make OPIOM compatible with a 1 Hz image acquisition rate, which is relevant for most dynamic studies in biology. Finally, since a difference in either $\sigma_{12}+\sigma_{21}$ or k_{21}^{Λ} of only tenfold is sufficient to achieve efficient discrimination (Figure 1b and Figure S12), it should permit multiplex observation of up to ten different fluorophores in a single emission channel.[21,22]

Received: September 11, 2014
Revised: November 5, 2014
Published online: January 21, 2015

Keywords: analytical methods · fluorescence · fluorescent probes · imaging agents · photochemistry

[1] B. Giepmans, S. Adams, M. Ellisman, R. Tsien, *Science* **2006**, *312*, 217–224.
[2] G. Marriott, R. M. Clegg, D. J. Arndt-Jovin, T. M. Jovin, *Biophys. J.* **1991**, *60*, 1374–1387.
[3] G. Marriott, S. Mao, T. Sakata, J. Ran, D. K. Jackson, C. Petchprayoon, T. J. Gomez, E. Warp, O. Tulyathan, H. L. Aaron, et al., *Proc. Natl. Acad. Sci. USA* **2008**, *105*, 17789–17794.
[4] Y. Yan, M. E. Marriott, C. Petchprayoon, G. Marriott, *Biochem. J.* **2011**, *433*, 411–422.
[5] C. I. Richards, J.-C. Hsiang, D. Senapati, S. Patel, J. Yu, T. Vosch, R. M. Dickson, *J. Am. Chem. Soc.* **2009**, *131*, 4619–4621.
[6] C. I. Richards, J.-C. Hsiang, R. M. Dickson, *J. Phys. Chem. B* **2010**, *114*, 660–665.
[7] C. I. Richards, J.-C. Hsiang, A. M. Khalil, N. P. Hull, R. M. Dickson, *J. Am. Chem. Soc.* **2010**, *132*, 6318–6323.
[8] C. Fan, J.-C. Hsiang, A. E. Jablonski, R. M. Dickson, *Chem. Sci.* **2011**, *2*, 1080.
[9] C. Fan, J.-C. Hsiang, R. M. Dickson, *ChemPhysChem* **2012**, *13*, 1023–1029.
[10] A. E. Jablonski, J.-C. Hsiang, P. Bagchi, N. Hull, C. I. Richards, C. J. Fahrni, R. M. Dickson, *J. Phys. Chem. Lett.* **2012**, *3*, 3585–3591.
[11] S. Sarkar, C. Fan, J.-C. Hsiang, R. M. Dickson, *J. Phys. Chem. A* **2013**, *117*, 9501–9509.
[12] J.-C. Hsiang, A. E. Jablonski, R. M. Dickson, *Acc. Chem. Res.* **2014**, *47*, 1545–1554.
[13] D. Alcor, V. Croquette, L. Jullien, A. Lemarchand, *Proc. Natl. Acad. Sci. USA* **2004**, *101*, 8276–8280.
[14] K. Zrelli, T. Barilero, E. Cavatore, H. Berthoumieux, T. Le Saux, V. Croquette, A. Lemarchand, C. Gosse, L. Jullien, *Anal. Chem.* **2011**, *83*, 2476–2484.
[15] T. Sandén, G. Persson, P. Thyberg, H. Blom, J. Widengren, *Anal. Chem.* **2007**, *79*, 3330–3341.
[16] J. Vogelsang, C. Steinhauer, C. Forthmann, I. H. Stein, B. Person-Skegro, T. Cordes, P. Tinnefeld, *ChemPhysChem* **2010**, *11*, 2475–2490.
[17] A. C. Stiel, S. Trowitzsch, G. Weber, M. Andresen, C. Eggeling, S. W. Hell, S. Jakobs, M. C. Wahl, *Biochem. J.* **2007**, *402*, 35.
[18] R. Ando, C. Flors, H. Mizuno, J. Hofkens, A. Miyawaki, *Biophys. J.* **2007**, *92*, L97–L99.
[19] R. Ando, H. Mizuno, A. Miyawaki, *Science* **2004**, *306*, 1370–1373.
[20] Y.-T. Kao, X. Zhu, W. Min, *Proc. Natl. Acad. Sci. USA* **2012**, *109*, 3220–3225.
[21] D. Bourgeois, V. Adam, *IUBMB Life* **2012**, *64*, 482–491.
[22] X. X. Zhou, M. Z. Lin, *Curr. Opin. Chem. Biol.* **2013**, *17*, 682–690.

